Supporting Information for Nanoporous Gold as a Highly Selective and Active Carbon Dioxide Reduction Catalyst

*Alex J. Welch[1,2], Joseph S. DuChene[1,2], Giulia Tagliabue[1,2], Artur Davoyan[1,2], Wen-Hui Cheng[1,2], and Harry A. Atwater[1,2]**

[1]Department of Applied Physics and Material Science, California Institute of Technology, Pasadena, CA 91125, USA.
[2]Joint Center for Artificial Photosynthesis, California Institute of Technology, Pasadena, CA 91125, USA.

Corresponding Author

* E-mail: haa@caltech.edu;

Experimental Methods:

Materials. Potassium carbonate (99.995%, Sigma Aldrich), Nitric Acid (18 M EMD Millipore Corporation), Si [p-type, 0-10 Ω cm, (100) orientation, 620 ± 25 μm thick, University Wafers], Au foil (99.9975%, 0.1 mm thick, Alfa Aesar), Pt foil (99.99% , 0.05 mm thick, Alfa Aesar) and Copper(II) sulfate (≥99%, Sigma Aldrich) were used without modification unless otherwise noted. The materials for electron beam deposition were ordered from Plasmaterials. The Au target was 99.99% pure with 3-6 mm random size pieces, Ag was 99.99% pure with 3-6 mm random size pieces, and Ti was 99.995% pure in 0.25" diameter pellets. All water used for experiments was deionized and filtered through a 0.22 μm Millipak Express 40, serial number 0826.

Fabrication of nanoporous Au (np-Au) films. An AMOD dual electron beam deposition system (System 02520, Angstrom Engineering) was used to fabricate all samples. First, Si substrates were cleaned by sonicating sequentially in acetone, isopropanol, and deionized water for five minutes each. The samples were then stored in deionized water until they were dried with N_2 prior to being placed in the electron beam deposition chamber. First, 2 nm of Ti was deposited at a rate of 1 Å/s, then 50 nm of Au was deposited at a rate of 2 Å/s. Next, Au and Ag were co-deposited at a rate of 2Å/s and 6Å/s, respectively, to create a 25% Au and 75% Ag alloy. Over the course of the deposition the partial pressure of the chamber would rise from ~10^{-7} torr to ~10^{-6} torr and the temperature would rise from 20 °C to 60 °C for a 1μm thick sample. If the samples were being etched at room temperature they were then placed in a beaker of 70 wt.% HNO_3 for 10 min. After this time had elapsed, they were rinsed with deionized water 10 times before being dried with N_2.

Scanning Electron Microscopy (SEM) characterization. The fabricated samples were imaged in a Nova200 Nanolab Dualbeam FIB/SEM with an acceleration voltage of 15 keV and spot size of 3. To image a cross section of the film, samples were cracked with a diamond scribe and placed at a 90° orientation relative to the electron beam.

Helium Focused Ion Beam (HFIB) characterization. The fabricated samples were imaged in a Zeiss HFIB with an acceleration voltage of 30 kV, beam current between 1-3 pA , working distance of 8 mm, and a scan dwell time of 6.5 μs.

X-ray diffraction (XRD) characterization. XRD spectra were taken using an X'PERT-PRO MRD Serial # DY3178 made by PANalytic. The scan went from 30° to 120°. The voltage was 45 kV, current 40 mA and the beam attenuator was Ni 0.125 mm automatic.

Cu Underpotential Deposition (Cu UPD) of Au films. The surface area of the np-Au was determined using Cu UPD. A $CuSO_4$ solution (0.1 M) in 0.5 M H_2SO_4 was prepared and used as the deposition bath for all Cu UPD experiments. The solution was bubbled with N_2 (Research grade from Airgas) for 30 min to remove dissolved O_2 from the solution prior to starting the experiment. The working electrode was a planar Au film or a np-Au film of various thicknesses with a Pt mesh counter electrode and a Ag/AgCl reference electrode. The potential of the

working electrode was swept from 450 mV to 50 mV vs. Ag/AgCl at a scan rate of 5 mV s^{-1}. A total of three to five electrodes were measured at each thickness ranging from 100 nm to 1.6 μm and the electrochemical surface area enhancement was obtained by taking the average surface area of the np-Au film relative to that of a planar Au film of known geometrical surface area.

Electrocatalytic CO_2 reduction reaction (CO_2RR) experiments. A two-compartment electrochemical cell made of polyether ether ketone (PEEK) was used to perform CO_2RR experiments. A volume of 2 mL of 50 mM K_2CO_3 was added to each compartment, which were separated by an anion exchange membrane (AGC, Selemion AMV). The np-Au film served as the working electrode with a Ag/AgCl leakless reference electrode and a Pt foil counter electrode. The Pt foil was soaked in 10 wt.% HNO_3 for 1 h and then flame annealed to remove contaminants before each experiment. The flame annealing process entails holding a flame to the foil until it glows red then rinsing the foil in water and drying. This process is repeated twice. The same procedure was also applied to the Au foil before testing. CO_2 saturated 50 mM K_2CO_3 (pH 6.8) was prepared by bubbling CO_2 (Research grade from Airgas) into the electrolyte for 30 min prior to experiments. Each electrolyte compartment was bubbled with CO_2 at a rate of 5 SCCM through a fine glass dispersion frit to maximize the speed of delivery of CO_2 into solution. The outflowing gas was sent through a flow meter to check that the flow of CO_2 in and out of the cell was the same, ensuring that it was thoroughly sealed against gas leaks. The outflowing gas was sent through a vapor trap to remove all water from the air before it was fed into a (SRI-8610) gas chromatograph.

All experiments were performed at room temperature with a Biologic VSP-300 potentiostat. All potentials were converted to the reversible hydrogen electrode (RHE) scale using the equation: E vs. RHE = E vs. Ag/AgCl + 0.197 V + 0.059 V pH^{-1} × solution pH. Before each experiment, potentiostatic electrochemical impedance spectroscopy (PEIS) was performed to determine the solution resistance of the cell, which was typically between 30 – 60 Ω. The applied electrochemical potential was then compensated by 85% using iR compensation of the potentiostat. The electrochemical cell was dismounted and rinsed multiple times after each experiment and then stored in 10 wt.% HNO_3. Before using the cell for the next experiment, it was sonicated for 10 min in water at least 4 times.

Analysis of chemical products. To analyze the chemical products, the electrode was held at the desired potential for at least 2 h allowing for the completion of eight gas chromatography measurements. The gas chromatograph (SRI-8610) used a Hayesep D column and a Molsieve 5A column with N_2 as the carrier gas. The gaseous products were detected using a thermal conductivity detector (TCD) for CO detection and a flame ionization detector (FID) equipped with a methanizer for H_2 detection. Quantitative analysis of gaseous products was based on calibration with several gas standards over many orders of magnitude in concentration. To measure liquid products, the electrolyte on the anode and cathode were sampled at the end of the run and tested with high performance liquid chromatography (HPLC). However, no liquid products were ever observed. Between different potential experiments all of the electrolyte was removed and

then the cell was rinsed three times with water before new electrolyte was add and bubbled with CO_2.

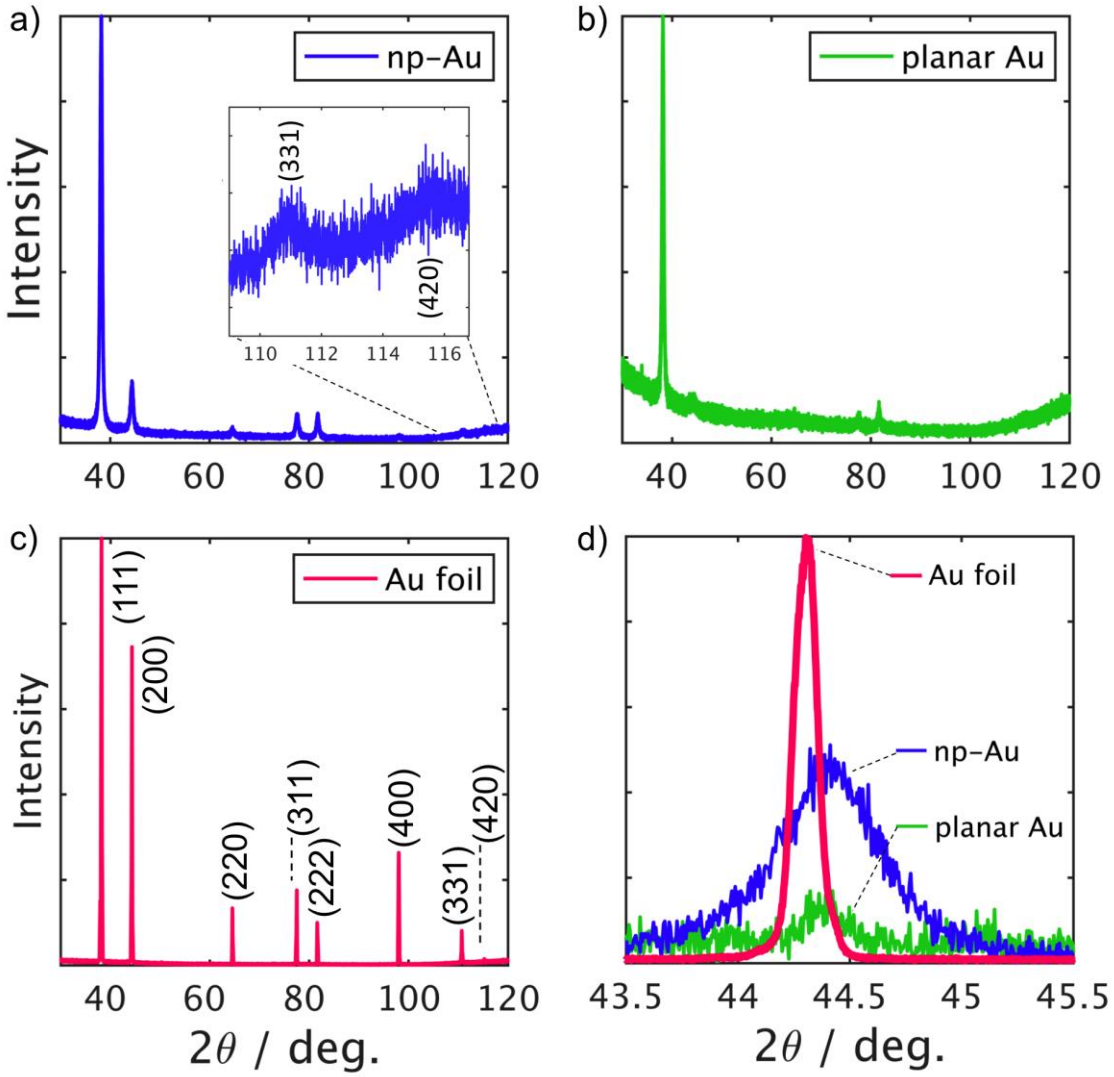

Figure S1. XRD spectra of (a) RT np-Au (~800 nm thick) on a glass substrate, (b) planar Au film on glass, and (c) Au foil after flame annealing. (d) Zoom-in of (200) peak where planar Au and np-Au have been increased by 20x. From the XRD it is evident that the planar Au film is highly oriented in the (111) orientation. The data also shows that the full width half max of the np-Au is much larger than that of the Au foil, indicating that the np-Au has smaller grains.

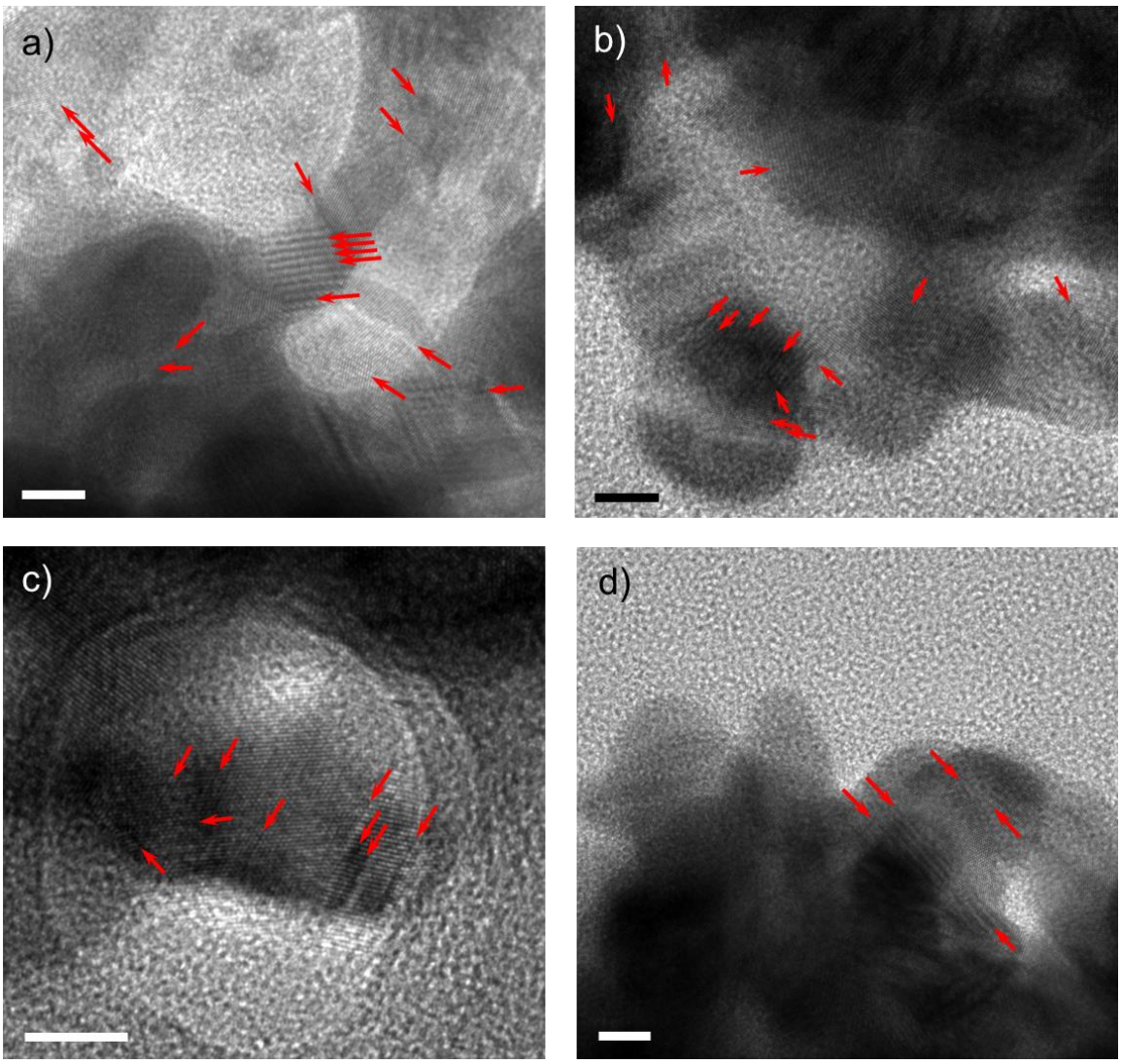

Figure S2. Bright field transmission electron microscopy (TEM) images of RT np-Au film. The red arrows denote grain boundaries. All scale bars represent 5 nm.

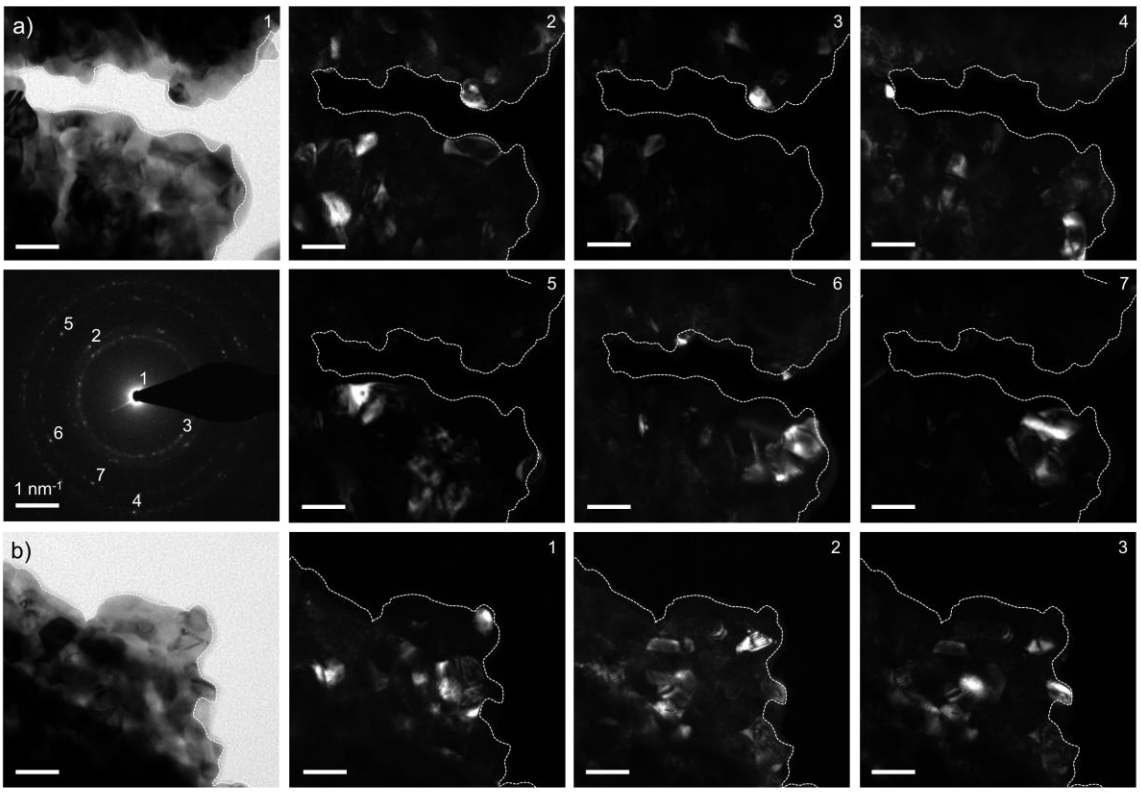

Figure S3. Transmission electron microscopy (TEM) analysis of RT np-Au films. (a) Bright-field TEM of a particular region of the np-Au film along with the corresponding selected area electron diffraction (SAED) pattern below it. The dark-field TEM images numbered 1-7 correspond to the spots numbered in the SAED pattern. (b) Bright-field TEM image of np-Au film along with dark-field TEM images numbered 1-3. All scale bars in all TEM images represent 20 nm.

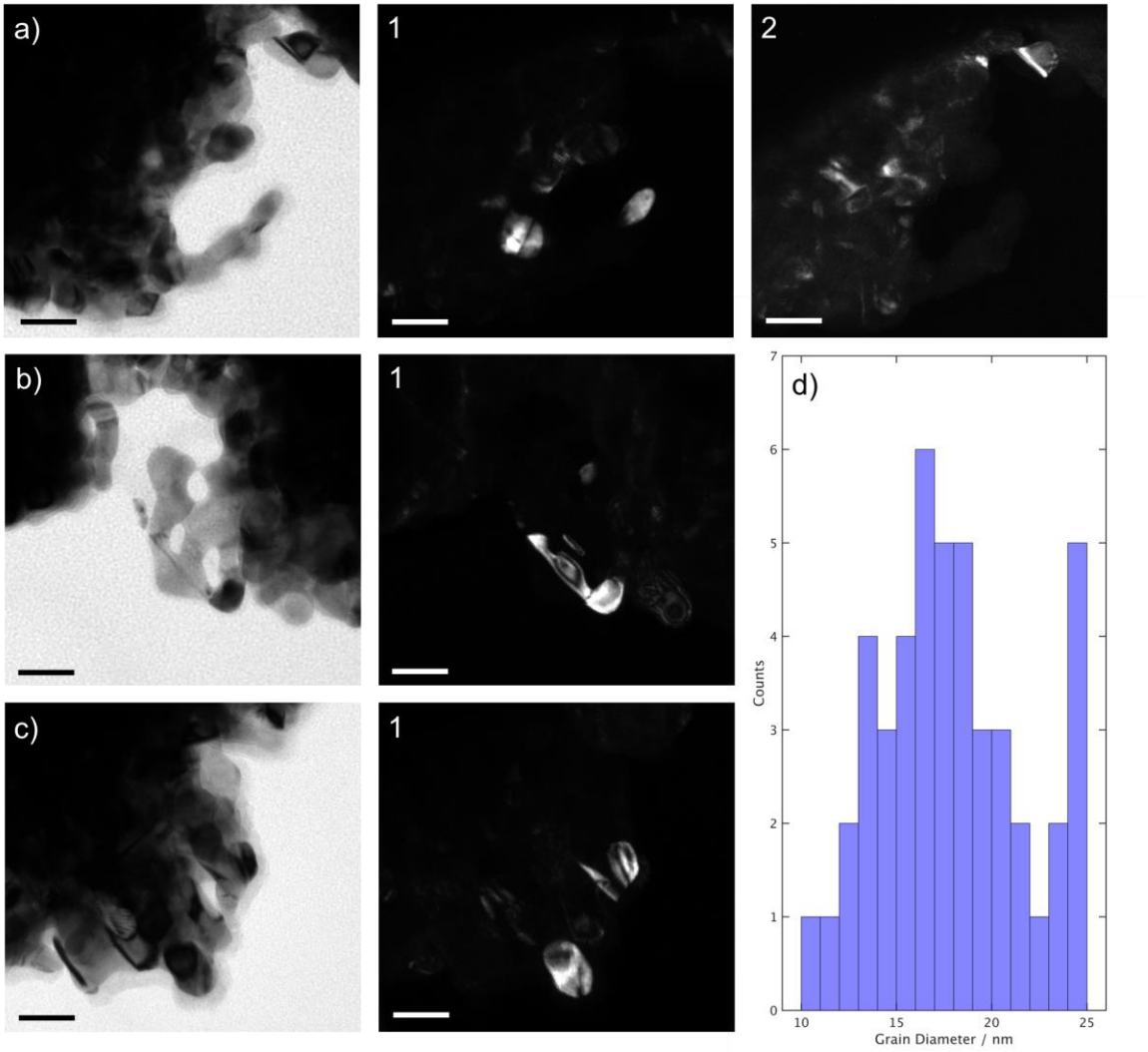

Figure S4. Transmission electron microscopy (TEM) analysis of RT np-Au films. (a-c) Bright-field TEM image of a particular region of the np-Au film along with the corresponding dark-field TEM image obtained from the same region of the np-Au film. All scale bars in all TEM images represent 20 nm. (d) Size distribution histogram of grain sizes obtained from analysis of dark-field TEM images.

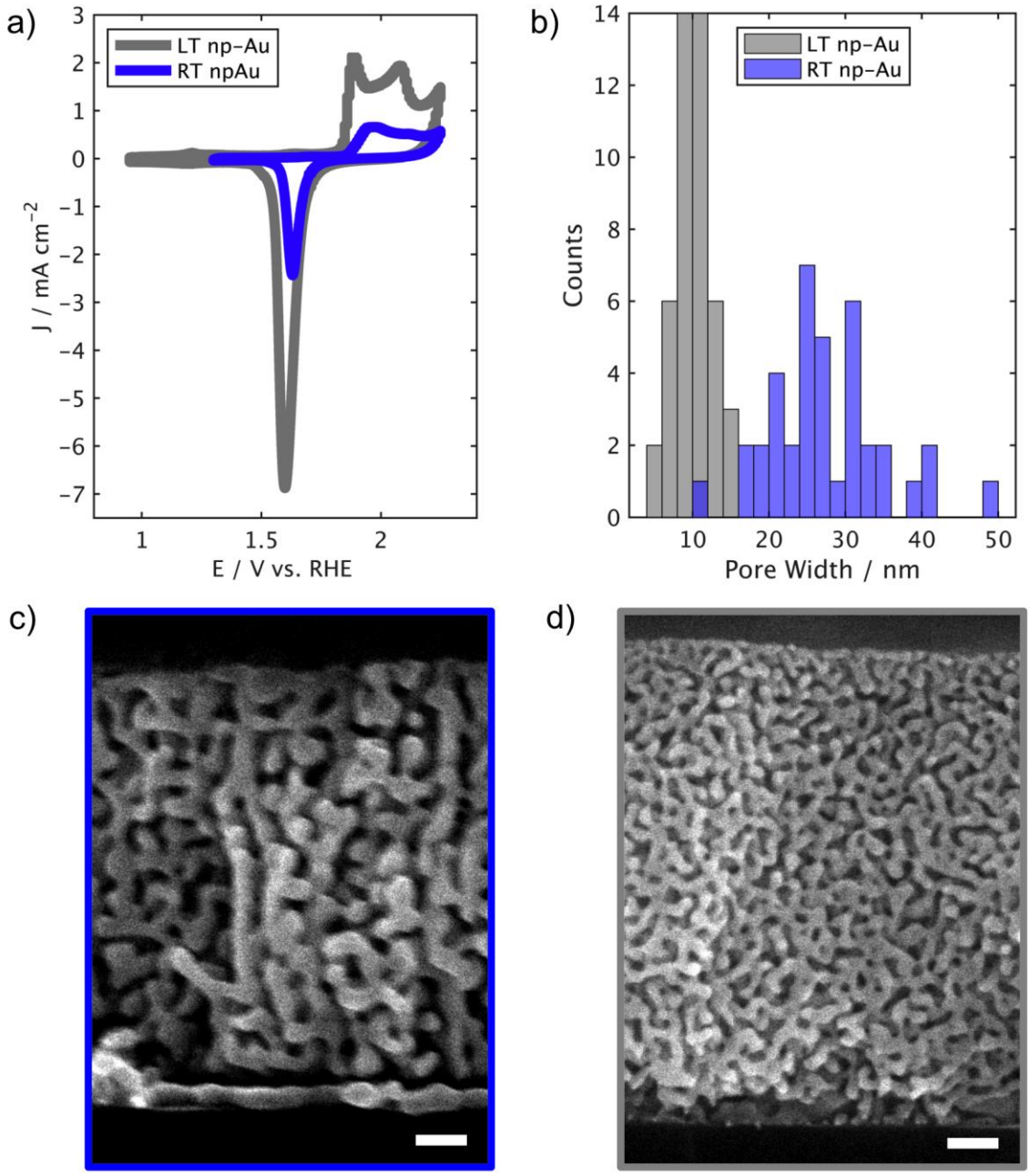

Figure S5. (a) Cyclic voltammetry of LT np-Au (grey curve) and RT np-Au (dark blue curve) in 0.5 M H_2SO_4 obtained at a scan rate of 50 mV s^{-1}. From these data we can determine that the LT sample has ~3x greater electrochemical surface area as compared to the RT sample. (b) shows a histogram of pore widths measured on these two samples at three different locations on the sample. Representative SEM cross-section images of (c) RT np-Au and (d) LT np-Au films. The scale bars on both images correspond to 100 nm. These images correspond to the actual electrodes used for electrochemical tests involving different electrolyte concentrations.

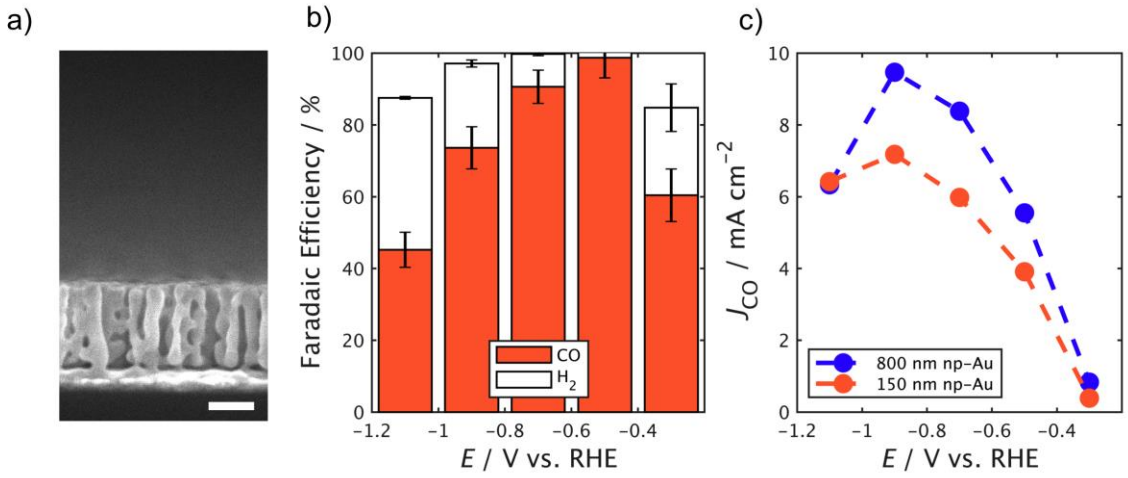

Figure S6. (a) SEM cross-section image of ~150 nm-thick RT np-Au film. The scale bar represents 100 nm. (b) Faradaic efficiency as a function of applied potential (*E*) for 150 nm-thick RT np-Au film. (c) Partial current density for CO (J_{CO}) from a 150 nm-thick and ~800 nm-thick RT np-Au sample. Considering the 4x smaller surface area of the thinner film, the relative J_{CO} between the two films is unexpected. We hypothesize that this is due to mass transport limitations.

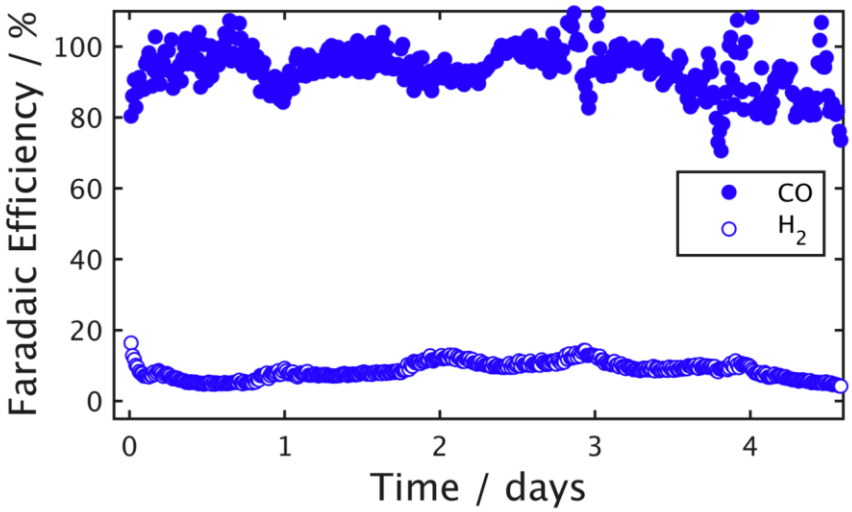

Figure S7. Extended electrochemical stability data for a RT np-Au film (~800 nm thick). The Faradaic efficiency for CO (filled points) and H_2 (open points) was measured every 15 min via gas chromatography over the course of 110 h at an applied potential of E = –0.5 V_{RHE} with iR compensation.

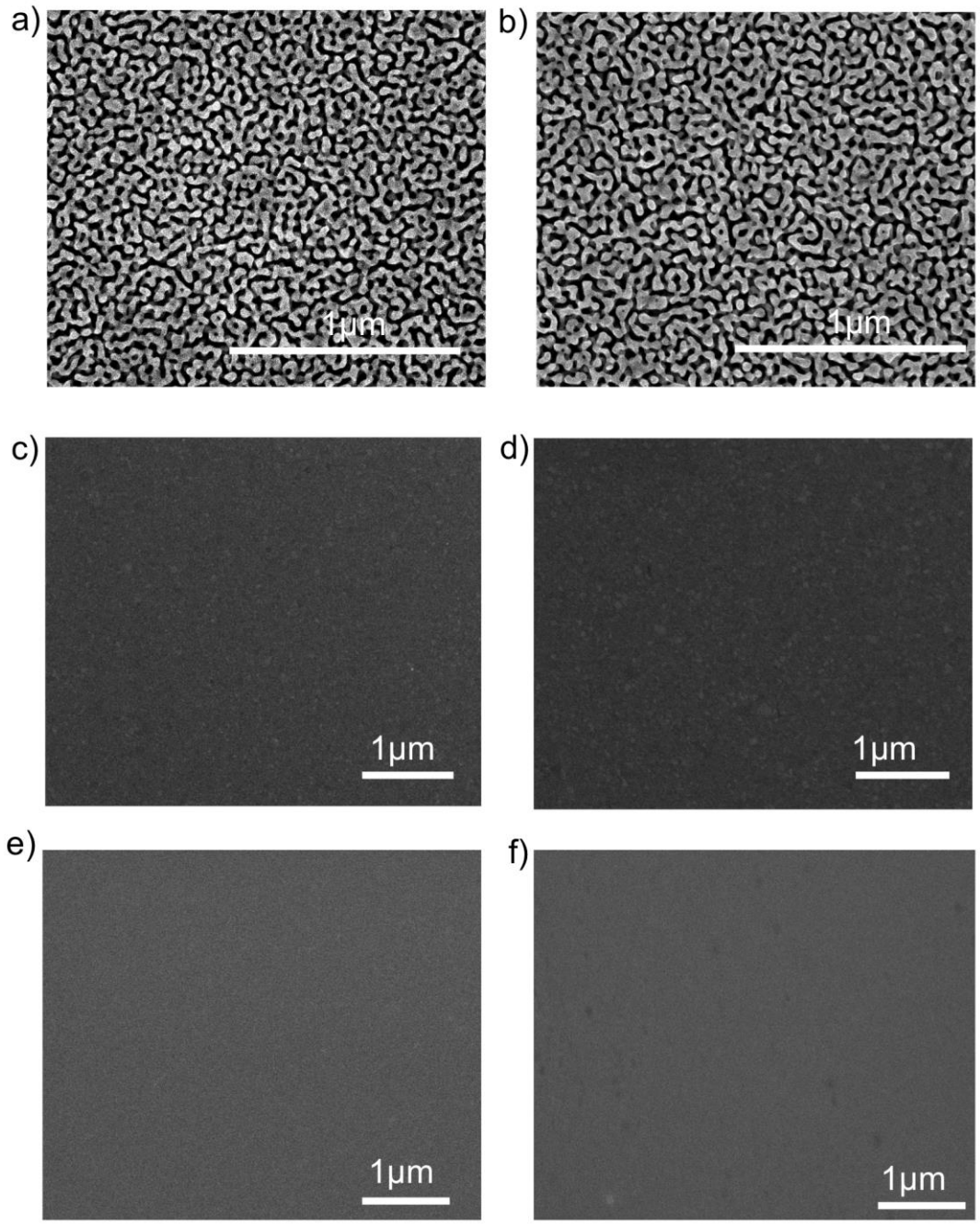

Figure S8. (a,b) SEM images of a ~800 nm thick RT np-Au film (a) before and (b) after testing for 110 h at −0.5 V vs. RHE. (c,d) SEM images of a planar Au film (c) before and (d) after testing for 24 h at −0.5 V vs RHE. (e,f) SEM images of a Au foil (e) before and (f) after testing for 24 h at −0.5 V vs RHE. There is no visible difference between any of the planar samples before and after testing. In the np-Au sample there is some minor coarsening of the ligaments, but no significant changes to the film morphology are observed.

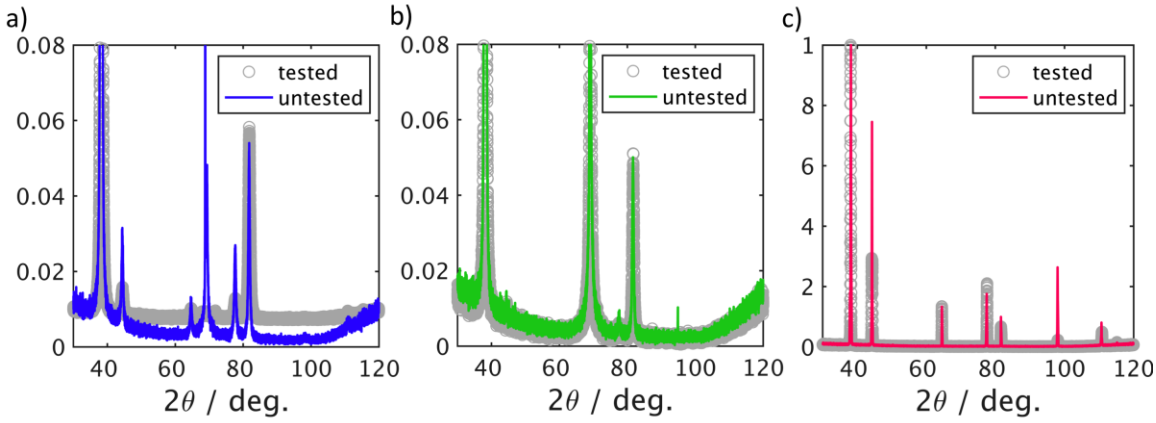

Figure S9. XRD spectra of Au films before and after 24 h of testing for (a) ~800 nm thick RT np-Au film, (b) planar Au film, and (c) Au foil. The peak at 68° in the RT np-Au film and the planar Au film is due to the Si substrate. In Fig. S1, the XRD patterns were collected from films supported on a glass substrate to avoid the peak from the Si substrate. Negligible differences were observed between Au peaks obtained from on Si vs. glass substrates.